

Automatic accuracy management of quantum programs via (near-)symbolic resource estimation

Giulia Meuli

EPFL, Lausanne, Switzerland
giulia.meuli@epfl.ch

Martin Roetteler

Microsoft, Redmond, United States
martinro@microsoft.com

Mathias Soeken

Microsoft, Zurich, Switzerland
mathias.soeken@outlook.com

Thomas Häner

Microsoft, Zurich, Switzerland
thhaner@microsoft.com

Abstract

When compiling programs for fault-tolerant quantum computers, approximation errors must be taken into account. We propose a methodology that tracks such errors automatically and solves the optimization problem of finding accuracy parameters that guarantee a specified overall accuracy while aiming to minimize a custom implementation cost.

The core idea is to extract constraint and cost functions directly from the high-level description of the quantum program. Then, our custom compiler passes optimize these functions, turning them into (near-)symbolic expressions for (1) the total error and (2) the implementation cost (e.g., total gate count). All unspecified parameters of the quantum program will show up as variables in these expressions, including accuracy parameters. After solving the corresponding optimization problem, a circuit can be instantiated from the found solution.

We develop two prototype implementations, one in C++ based on Clang/LLVM, and another using the Q# compiler infrastructure. We benchmark our prototypes on typical quantum computing programs, including the quantum Fourier transform, quantum phase estimation, and Shor’s algorithm.

Keywords Quantum algorithms, approximation errors, language support, resource estimation

1 Introduction

There exists a wide range of quantum algorithms that promise asymptotic speed-ups with respect to their classical counterparts. Application domains include cryptography [6, 29], machine learning [18], material science [25], and quantum chemistry [3, 24]. However, concrete resource estimates for problems at which quantum computers are expected to outperform their classical counterparts remain scarce. To carry out such resource estimates, several quantum programming languages and toolchains have been developed such as Q# [36], Quipper [16], Scaffold/ScaffCC [21], Qiskit [13], ProjectQ [34], and QuRE [35]. Some of these frameworks provide domain-specific languages with the necessary abstractions, libraries, simulators, and in some cases cloud

access to small-scale quantum computers. Despite the availability of these languages, there is still a significant amount of manual work involved in resource estimation [31, 32]—one reason being the lack of built-in support for handling approximation errors.

Why do approximation errors occur in quantum programs in the first place? We discuss three main sources of errors in this paper, however, the framework is extensible to other sources of error:

1. Synthesis errors. Due to the discrete nature of the commonly used fault-tolerant instruction sets (and indeed, it is known that any universal fault-tolerant instruction set necessarily must be discrete [26]), it cannot be avoided to introduce approximation errors. For instance, consider a rotation around the Z -axis such as

$$R_Z(\theta) = \begin{bmatrix} e^{-i\theta/2} & 0 \\ 0 & e^{i\theta/2} \end{bmatrix},$$

which can be defined for any $\theta \in [0, 4\pi)$. Such rotations can only be implemented exactly for a discrete subset of the interval $[0, 4\pi)$, as gates have to be expressed as words of finite length over any universal set of generators. It should be noted that there is a mathematical function that expresses the length of the approximating word in terms of an approximation error, which we label ϵ_R . This mathematical function depends on the concrete synthesis algorithm used to perform the factorization into fault-tolerant instructions. State-of-the-art synthesis algorithms lead to a cost (e.g., number of T gates, where $T = e^{i\pi/8} R_Z(\pi/4)$) that is proportional to $\log_2(\epsilon_R^{-1})$.

2. Phase estimation errors. An important technique in quantum computing is to extract estimates of an eigenvalue λ of an operator U [22, 33]. A common method to achieve this works by preparing an eigenstate $|\psi_\lambda\rangle$ of U and then applying powers U^{2^i} , for $i = 0, \dots, k$ to the eigenstate $|\psi_\lambda\rangle$. This application is done conditionally on the value of a reference system and allows us to extract the $k+1$ most significant bits of the eigenvalue. As λ can in principle be any complex number of the form $\lambda = e^{i\alpha}$, where $\alpha \in [0, 2\pi)$, the particular choice of k introduces an approximation error and

limits how precisely we can estimate λ . We label the resulting approximation error ϵ_{QPE} .

3. General algorithmic errors. Some quantum programs are part of a parametric family of programs that gracefully degenerate with a reduction of the parameters. A concrete example for such a family of programs is the quantum Fourier transform [33]. While the transformation itself can be implemented exactly and with no approximation error over a gate set that includes continuous rotations such as $R_Z(\theta)$ for arbitrary $\theta \in [0, 4\pi)$, it is possible to approximate the transformation by selectively dropping some of the rotations that occur, in particular by “pruning” values of θ that are very close to 0. One such pruning method is well known [10] and allows us to drop many of the $O(n^2)$ rotations that a simple implementation of the Fourier transform requires and just retain $O(n \log n)$ rotations, while still maintaining an excellent approximation. We call the resulting approximation error ϵ_{QFT} in the paper. Another example of algorithmic error comes from formulas that are known to converge to a target program when taking the limit, e.g., of alternations of other, typically smaller and simpler programs. An example for the latter is the so-called Trotter formula, a well-known identity to implement an approximation to $e^{i(A+B)}$ for Hermitian matrices A and B , from the knowledge of implementations of e^{iA} and e^{iB} . The resulting approximation error is called ϵ_{TE} in the paper.

Overview of our approach. A quantum program can be expressed at a high level of abstraction using any of the languages and frameworks mentioned above. Instead of specifying quantum circuits at the level of single- and two-qubit quantum gates, these languages provide abstract primitives such as *quantum Fourier transform* and *quantum phase estimation*, which can be used when implementing a quantum algorithm. Once the target machine has been specified, a compiler is used to translate this high-level description of the quantum program to low-level hardware-specific gates, such as the Clifford+ T gate set [1], which can be implemented fault-tolerantly on several scalable quantum computer architectures [8].

At any point in the quantum program and during compilation, various approximations may be necessary, such as the ones described thus far. With existing languages, programmers must manually keep track of all of these approximation errors. In addition, they must tune the parameters of their implementation to keep the total error beneath a given threshold. To guarantee this, they must derive the resulting error bounds manually.

To address this issue, our methodology introduces language support into existing quantum programming languages to allow programmers to deal independently with the approximation errors introduced by each subroutine. The job of inferring how all introduced approximation errors interact is thus transferred from the programmer to the compiler.

Our methodology automatically infers an error bound for the overall quantum program and then selects appropriate values for each of the program’s accuracy parameters to simultaneously (1) satisfy a user-specified overall tolerance and (2) reduce the required quantum resources.

More specifically, our methodology supports:

1. given the desired approximation error, determining the assignment of accuracy parameters that guarantees the given approximation error while aiming to minimize the number of operations;
2. given a maximal operation count, determining the assignment of accuracy parameters that yield at most the given operation count while aiming to reduce the total approximation error.

The automatic optimization of accuracy parameters is carried out by solving an optimization problem before a quantum circuit is generated. The constraint and cost functions describing the optimization problem are extracted by the compiler directly from the source code of the quantum program. Then, before execution, the optimized accuracy parameters are fed into the main program.

Finding a suitable assignment of accuracy parameters using, e.g., simulated annealing, requires hundreds of evaluations of both constraint and cost functions. Hence, our methodology has to lean on a fast method to estimate resource requirements and the total approximation error. Available methods, e.g., in Q#, estimate resources by actually generating quantum circuits from completely specified programs and then counting the generated gates. Hence, their runtime will increase with increasing problem size, making them ill-suited to cost function evaluation in a simulated annealing procedure, as we will show in Section 8.

Instead, we propose fast symbolic methods that extract a symbolic expression for the desired cost or constraint function (total approximation error or number of gates) directly from the source code of the quantum program. The resulting expressions feature variables that correspond to the various parameters of the program, including accuracy parameters. The symbolic approach does not need to execute the complete control flow of the quantum program to get an estimate, hence it provides a much faster solution that is viable even for application-scale programs.

Our two prototypes both implement a symbolic approach for resource and error estimation. Since the resulting expressions may theoretically still contain some residual code that must be executed (e.g., certain if-else statements), we refer to them as being (*near-*)*symbolic*. However, both our prototypes generate fully symbolic expressions for all the examples in this paper.

Contributions. To the best of our knowledge, we are the first to present a quantum programming framework that provides built-in support for automatic accuracy management. Our methodology automatically selects accuracy parameters

such that the overall error is at most equal to a user-specified value while aiming to reduce the quantum resource requirements, or vice versa. As the interplay between the various approximation errors can be quite complicated, it can be difficult for a human to find the best trade-offs.

In addition, our approach for extracting *symbolic* resource estimates from the quantum program, and using them to specify and solve the optimization problem of tuning accuracy parameters, appears to be new. Some state-of-the-art methods exist to automate resource estimation. Examples are methods embedded in Q#, ProjectQ, and Quipper, which are based on circuit-description languages, and QuRE, which is capable of evaluating different technologies and error-correcting codes. Nevertheless, all these frameworks require *a priori* specified quantum circuits. Thus, they cannot be used to derive asymptotic estimates as a function of the input parameters of the algorithm, in contrast to the symbolic approach we propose.

Indeed, a salient feature is that we acquire symbolic estimates for the total error and gate count directly from the high-level description of a quantum program, without executing the control-flow. It is only after the final resource requirements and total approximation error are known that we instantiate a circuit using the determined accuracy parameters. This allows us to automatically evaluate the resource requirements of a given quantum program in an accuracy-aware fashion, without the overhead of having to execute the entire control-flow of the program.

We evaluate our framework with reference implementations in C++ and Q#, where in both cases we implemented new compiler passes to enable the new functionality. Finally, we validate and benchmark our methodology on quantum programs such as *quantum phase estimation* and *Shor's algorithm* [33]. We show that the runtime gap between the best previous methods and our symbolic method for resource and error estimation is *unbounded* as a function of the problem size.

Related work. In [19], a theoretical framework is presented to reason about erroneous behavior in quantum programs and analyze noise. That approach relies on an explicit representation of quantum states by means of density matrices. Therefore, a hypothetical implementation would not scale to programs that require significantly more than 20 qubits. In contrast, we provide an implementation of our theoretical framework and demonstrate that it is capable of handling application-scale quantum programs featuring thousands of qubits and billions of operations.

Our methodology also relates to the automatic approach presented in [28] for handling floating-point rounding errors in classical computing. This approach, called *Herbie*, is capable of locating sources of errors in the code and proposing candidate rewrites to improve the overall precision. Similarly, our approach locates and adapts accuracy parameters

to reduce the total error. While *Herbie* must be combined with other methods [4, 7, 11] to provide worst-case guarantees, our methodology proposes parameter assignments that guarantee the specified worst-case upper bound, assuming a correct implementation. We are not concerned with verifying actual correctness of the quantum program, but refer the reader, e.g., to [37].

Further related work is symbolic execution, which is widely used for code testing and for finding bugs. The method translates the given program into a logical formula in order to check some input properties. A relevant example is *veritest* [2], which alternates dynamic (DSE) and static (SSE) symbolic execution for testing. Similarly, we extract from a quantum program symbolic expressions for upper bounds on the total error and the gate count.

2 Quantum computing background

2.1 Quantum states

Quantum computers process information encoded in qubits. The quantum state of a qubit $|\phi\rangle$ (using *Dirac* or *bra-ket* notation) can be written as

$$|\phi\rangle = \alpha_0 |0\rangle + \alpha_1 |1\rangle,$$

where $\alpha_0, \alpha_1 \in \mathbb{C}$ are the complex probability amplitudes corresponding to the *computational basis states* $|0\rangle$ and $|1\rangle$, respectively, and $|\alpha_0|^2 + |\alpha_1|^2 = 1$. The computational basis states $|0\rangle$ and $|1\rangle$ may be associated with two-dimensional basis vectors $|0\rangle = \begin{pmatrix} 1 \\ 0 \end{pmatrix}$ and $|1\rangle = \begin{pmatrix} 0 \\ 1 \end{pmatrix}$. Single-qubit quantum gates (or quantum operations) can be written as 2×2 -dimensional complex unitary matrices. A matrix U is unitary if its conjugate transpose corresponds to its inverse: $UU^\dagger = U^\dagger U = \mathbb{1}$. When applying a quantum gate to a single qubit, its new quantum state can be computed via a simple matrix-vector multiplication of the gate matrix and the two-dimensional amplitude vector $|\phi\rangle = \begin{pmatrix} \alpha_0 \\ \alpha_1 \end{pmatrix}$.

Similarly, an n -qubit quantum state may be described by a vector containing the 2^n amplitudes corresponding to all possible bitstrings of length n , or, using the *bra-ket* notation:

$$\sum_{x \in \mathbb{B}^n} a_x |x\rangle,$$

where $\sum_x |a_x|^2 = 1$. Quantum operations over n qubits are modeled by unitary matrices of size $2^n \times 2^n$.

Measuring all n qubits of the n -qubit state above results in a *collapse* of the superposition onto one of the computational basis states $|x\rangle$ with probability $|a_x|^2$.

2.2 Quantum gates

A quantum program consists of classical *and* quantum instructions [23]. While classical instructions are performed on the (classical) controller, the latter are performed on the quantum processing unit (QPU). In each step of the computation, the controller sends a sequence of quantum instructions to the QPU. After execution of each such sequence, the

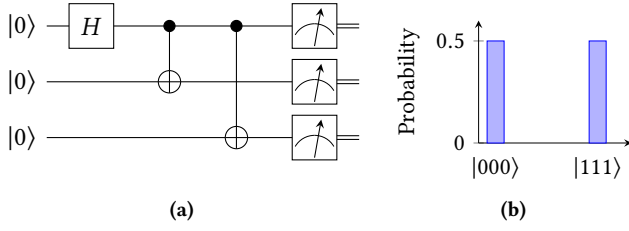


Figure 1. Example of a quantum circuit computing an entangled state (a) and the corresponding expected measurement outcomes (b).

QPU returns classical measurement results to the controller, which may use them to decide on the quantum instructions to perform next (if any).

The mentioned sequences of quantum instructions can be visualized using circuit diagrams, so-called *quantum circuits*.

Example 1. An example of a quantum circuit is shown in Fig. 1. This circuit generates a Greenberger–Horne–Zeilinger state on three qubits, i.e., the state

$$\frac{1}{\sqrt{2}}(|000\rangle + |111\rangle).$$

In a quantum circuit, each qubit is represented by a horizontal line. Operations are denoted by boxes or other symbols on the qubit(s) they are being applied to. Time advances from left to right. The first operation is a Hadamard gate (H) applied to the first qubit. In matrix notation,

$$H = \frac{1}{\sqrt{2}} \begin{pmatrix} 1 & 1 \\ 1 & -1 \end{pmatrix}.$$

Applying H to the first qubit maps $|000\rangle$ to $\frac{1}{\sqrt{2}}(|000\rangle + |100\rangle)$. The next gate is a controlled-NOT or CNOT,

$$\text{CNOT} = \begin{pmatrix} 1 & 0 & 0 & 0 \\ 0 & 1 & 0 & 0 \\ 0 & 0 & 0 & 1 \\ 0 & 0 & 1 & 0 \end{pmatrix},$$

which entangles the first with the second qubit by flipping the latter if the first qubit is $|1\rangle$. After the two CNOT gates, the three qubits are in the state $\frac{1}{\sqrt{2}}(|000\rangle + |111\rangle)$. Finally, all three qubits are measured. There is a 50% probability of measuring all 0s and a 50% probability of measuring all 1s.

Quantum programs can be written in one of the various languages and software frameworks for quantum computing, e.g., ProjectQ, Q#, Qiskit. All of these languages allow programmers to specify the quantum program in terms of high-level operations. They also provide methods to decompose such operations into the native gate set of the QPU. Different quantum architectures support different native operations. A common low-level instruction set is the so-called Clifford+ T gate set [1]. This instruction set includes the already mentioned CNOT gate and Hadamard gate H , as well

as the gates

$$X = \begin{bmatrix} 0 & 1 \\ 1 & 0 \end{bmatrix}, Y = \begin{bmatrix} 0 & -i \\ i & 0 \end{bmatrix}, Z = \begin{bmatrix} 1 & 0 \\ 0 & -1 \end{bmatrix}, T = \begin{bmatrix} 1 & 0 \\ 0 & e^{i\pi/4} \end{bmatrix}.$$

Here X , Y , and Z denote the Pauli matrices that, like CNOT and H , are Clifford gates, while T is a non-Clifford gate required to achieve universality. In a fault-tolerant setting, the T gate is particularly expensive to be applied. As a consequence, the T -count (number of T gates) is a good measure for the cost of a fault-tolerant implementation of a given quantum program [9, 15].

2.3 Error propagation in quantum circuits

Given a quantum program that executes a sequence of approximate quantum instructions, how do the approximation errors of these individual instructions compose?

In this section, we prove that an upper bound on the total approximation error can be derived by adding all individual approximation errors. As a consequence, our methodology produces quantum circuits with accuracy guarantees for quantum programs without measurement feedback. Note that this excludes programs that rely on repeat-until-success statements, i.e., loops that iterate until a certain measurement outcome is observed (see, e.g., [27]). Such cases can be handled separately using, e.g., an upper bound on the number of iterations.

Quantum circuits corresponding to feedback-free programs consist of a sequence of gates U_1, \dots, U_m , followed by a sequence of measurements M_1, \dots, M_k that produce a measurement outcome $m = x_i$ for a final state

$$|\psi\rangle = U_m \cdots U_1 |0\rangle^{\otimes N}$$

with probability

$$P(m = x_i) = |\langle x_i | \psi \rangle|^2.$$

Therefore, our methodology must ensure that the actual final state $|\tilde{\psi}\rangle$ is close to the desired final state $|\psi\rangle$ after all decompositions have been applied to U_1, \dots, U_m .

Let V_1, \dots, V_n be an approximate decomposition of the quantum program in terms of the gates supported by the target hardware, i.e.,

$$\| \underbrace{U_m \cdots U_1}_U - \underbrace{V_n \cdots V_1}_V \| \leq \varepsilon.$$

Then, $\| |\psi\rangle - |\tilde{\psi}\rangle \| = \| U |0\rangle^{\otimes N} - V |0\rangle^{\otimes N} \| \leq \varepsilon$, which guarantees that, with $|\psi\rangle = \sum_i a_i |x_i\rangle$ and $|\tilde{\psi}\rangle = \sum_i \tilde{a}_i |x_i\rangle$,

$$\begin{aligned} |a_i - \tilde{a}_i| &= \sqrt{|a_i - \tilde{a}_i|^2} \\ &\leq \sqrt{\sum_i |a_i - \tilde{a}_i|^2} \\ &\leq \varepsilon. \end{aligned}$$

Therefore, it is sufficient that our methodology guarantees

$$\|U - V\| \leq \varepsilon.$$

In the process of translating the quantum program to the native gate set, several decompositions are applied that introduce approximation errors. Let U be a quantum operation being approximated by the decomposition into W_1, \dots, W_t . The decomposition introduces at most ε_U if $\|U - (W_t \cdots W_1)\| \leq \varepsilon_U$, assuming that all W_i are implemented exactly. Now, combining multiple such approximate implementations \tilde{U}_i of U_i such that $\|U_i - \tilde{U}_i\| \leq \varepsilon_i$ yields a total error of at most $\sum_i \varepsilon_i$ [17].

Therefore, it is possible to derive recursively-defined expressions for the error $E(U, \varepsilon_U)$ and the total gate count $T(U, \varepsilon_U)$ [17]:

$$E(U, \varepsilon_U) = \varepsilon_U + \sum_{W \in D(U, \varepsilon_U)} E(W, \varepsilon_W) f_W(\varepsilon_U)$$

$$T(U, \varepsilon_U) = \sum_{W \in D(U, \varepsilon_U)} T(W, \varepsilon_W) f_W(\varepsilon_U)$$

where $D(U, \varepsilon_U)$ is the set of gates in the ε_U -approximate decomposition of U and $f_W(\varepsilon_U)$ denotes the number of W operations in the decomposition. Looking at these expressions, it is clear that an upper-bound on the total error can be computed very similarly to counting gates.

In conclusion, choosing all $\varepsilon_{(\cdot)}$ in the expression for

$$E(U_{Main}, \varepsilon_{U_{Main}})$$

such that $E(U_{Main}, \varepsilon_{U_{Main}}) \leq \varepsilon$, ensures that the measurement probability amplitude for a given bit-string changes by at most ε .

3 Sample quantum programs

3.1 Simulating time-evolution of operators

Being a quantum system, a quantum computer can be programmed to simulate other quantum systems. This can be used, e.g., to elucidate chemical reaction mechanisms [31].

Given the quantum-mechanical Hamiltonian \mathcal{H} which describes the system being studied, the time evolution of the system can be simulated by implementing the *time-evolution operator* $U = e^{-i\mathcal{H}t}$. The time-evolved quantum state can then be obtained by applying U to the initial state $|\psi(0)\rangle$:

$$|\psi(t)\rangle = e^{-i\mathcal{H}t} |\psi(0)\rangle.$$

In order to implement the time-evolution operator on a quantum computer, it needs to be decomposed into the native gate set, e.g., Clifford+ T . Different decomposition methods are available, each one scaling differently with the targeted precision ε_{TE} : polynomial for the Trotter decomposition method, logarithmic for the linear combination of unitaries (LCU) [3, 30].

Example 2. Consider the Hamiltonian of a 1D transverse-field Ising model (TFIM)

$$\mathcal{H} = -J \underbrace{\sum_{\langle i,j \rangle} Z^i Z^j}_{\mathcal{H}_1} - h \underbrace{\sum_i X^i}_{\mathcal{H}_2},$$

where \mathcal{H}_1 defines the interaction of adjacent spins with periodic boundary conditions and \mathcal{H}_2 defines the interaction of the system with the external transverse field.

Using a second-order Trotter-Suzuki decomposition, the time-evolution operator under this Hamiltonian can be written as

$$e^{-i\mathcal{H}t} \approx (e^{-i\mathcal{H}_1 \frac{t}{2M}} e^{i\mathcal{H}_2 \frac{t}{M}} e^{-i\mathcal{H}_1 \frac{t}{2M}})^M.$$

The number of Trotter steps M will be chosen according to the desired accuracy ε_{TE} . In particular, for this second-order Trotter decomposition we have that M is proportional to $1/\sqrt{\varepsilon_{TE}}$ [31]. Each Trotter step can be implemented using CNOT and $R_Z(\theta)$ gates. The latter being a gate that applies a rotation equal to the angle θ around the z-axis. Considering Clifford+ T as the native gate set, each rotation has to be synthesized or decomposed in terms of these gates. As not every rotation can be realized exactly using this gate library, rotation synthesis also introduces an error. Given a target approximation error ε_R , the number of T gates per rotation will be proportional to $\log_2\left(\frac{1}{\varepsilon_R}\right)$ when using the best currently available methods [14, 27].

Thus, to express the time-evolution operator we need to take into account two inter-dependent approximation errors, namely ε_{TE} and ε_R .

3.2 Quantum Fourier transform

The quantum Fourier transform (QFT) is an algorithm that performs the Fourier transform of quantum mechanical amplitudes. QFT is implemented as a linear operator that applies the following unitary transformation on a basis state $|j\rangle$ [26]:

$$|j\rangle \mapsto \frac{1}{\sqrt{N}} \sum_{k=0}^{N-1} e^{2\pi i j k / N} |k\rangle$$

The effect of the transform on an arbitrary state can be described using a product representation that maps $|j_1, \dots, j_n\rangle$ to

$$\frac{(|0\rangle + e^{2\pi i 0 \cdot j_n} |1\rangle)(|0\rangle + e^{2\pi i 0 \cdot j_{n-1} j_n} |1\rangle) \dots (|0\rangle + e^{2\pi i 0 \cdot j_1 j_2 \dots j_n} |1\rangle)}{2^{N/2}}$$

where $0.j_1 j_2 \dots j_m$ is the binary expansion $j_1/2 + j_2/4 + \dots + j_m/2^{m-1}$. This representation has a direct correspondence to the circuit implementation of the quantum Fourier transform shown in Fig. 2. The circuit is composed of n steps, one for each qubit. In each step, for each qubit, a Hadamard gate is applied, followed by a series of rotation gates controlled by all remaining qubits.

In this work, we will largely refer to an approximate version of QFT (AQFT) in which the number of rotations is reduced according to the desired approximation error ε_{QFT} .

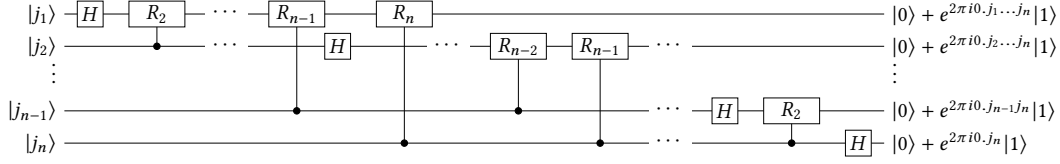


Figure 2. Efficient circuit computing the quantum Fourier transform.

This is done by pruning rotations with small angles. In particular, for each qubit j_i with $1 \leq i < n$ a maximum of

$$l = \lceil \log_2(n/\varepsilon_{QFT}) \rceil + 3$$

controlled-rotations is applied [10].

The quantum Fourier transform enables the *quantum phase estimation* algorithm and has a key role in the solution of many relevant problems, e.g., the *integer factorization* problem.

3.3 Quantum phase estimation

Once time-evolution under the Hamiltonian \mathcal{H} is implemented, one may perform measurements similar to experiments with the actual system. Quantum computing, however, allows us to achieve a quadratic advantage over repeated measurement and sampling via quantum phase estimation (QPE). Given a state with large overlap with the ground state $|\psi_0\rangle$ of the Hamiltonian, this algorithm allows us to determine the ground state energy E_0

$$\mathcal{H}|\psi_0\rangle = E_0|\psi_0\rangle.$$

One of several possible implementations of QPE [26] is shown in Fig. 3. The measurement outcomes of the top $k + 1$ qubits yield a $k + 1$ -bit approximation to the phase due to time-evolution. More precisely, the number of qubits to choose n_{QPE} depends on the desired accuracy *and* the probability p of a successful measurement as follows

$$n_{QPE} = n + \left\lceil \log \left(2 + \frac{1}{2(1-p)} \right) \right\rceil,$$

where n is the desired accuracy in number of bits.

The number of controlled time-evolution unitaries required for QPE to succeed with $p = 0.5$ and accuracy ε_{QPE} may thus be bounded by $2^{n_{QPE}} - 1 \leq 16\pi/\varepsilon_{QPE}$.

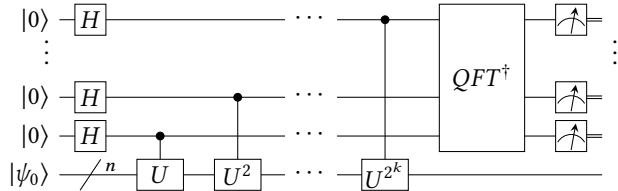


Figure 3. Quantum circuit performing quantum-phase estimation on an n -qubit system with an accuracy of $k + 1$ bits.

Not only does QPE allow one to infer the ground state energy if the ground state is known, but it also collapses a non-eigenstate input $|\phi\rangle$ to the i -th eigenstate $|\psi_i\rangle$ of the Hamiltonian H with probability $|\langle\psi_i|\phi\rangle|^2$.

In terms of accuracy, it is important to distinguish between the different applications of QPE. If QPE is used to determine only the energy, i.e., $|E_0 - \tilde{E}_0| \leq \varepsilon$ is required, then it is sufficient to implement time-evolution such that $\|U - \tilde{U}\| \leq \varepsilon - \varepsilon_{QPE}$. However, if the goal is to prepare the ground state, i.e., $\|\psi_0 - \tilde{\psi}_0\| \leq \varepsilon$, then $\|U - \tilde{U}\| \leq \frac{\varepsilon - \varepsilon_{QPE}}{2^{n_{QPE}} - 1}$ is sufficient (both via triangle inequality). Distinguishing these cases clearly has a great impact on the resulting resource requirements.

4 Language support for accuracy management

Since large-scale quantum computers are not yet available, resource estimation is a crucial feature of any software framework for quantum computing. Typically, such resource estimation is performed by compiling the quantum program into the chosen target gate set and then executing the resulting circuit on a classical simulator that counts native operations (instead of executing them). For this to be possible, however, all the parameters of the program, including accuracy parameters for each subroutine, must be determined.

Existing quantum programming languages do not offer built-in support for accuracy management. Consequently, it is very cumbersome to implement large-scale quantum algorithms in an accuracy-aware fashion. Thus, despite the availability of a wide range of quantum programming languages, resource estimates are still computed (semi-)manually, taking care of accuracy parameters using pen and paper [31, 32].

The main difficulty when selecting appropriate accuracy parameters is that parameters at a higher level of abstraction have an effect on the ones at lower levels, as illustrated by the following example:

Example 3. Consider QPE on $U = R_Z(\alpha) := e^{-i\frac{\alpha}{2}Z}$ and the target gate set Clifford+T. The number of phase-estimation qubits n_{QPE} depends on the desired precision of the phase (and the probability of success). At the lowest level, the various $U^{2^i} = R_Z(\alpha_i)$ are decomposed into a sequence of Clifford+T gates featuring $O(\log \frac{1}{\varepsilon_r})$ T gates. To achieve an overall target accuracy ε , ε_r must be chosen such that $\varepsilon_{QPE} + \varepsilon_R \leq \varepsilon$, where ε_R denotes the error introduced by all rotations in the quantum

circuit. Since ϵ_{QPE} affects the number of rotations in the circuit, ϵ_r must be chosen as a function of ϵ_{QPE} .

In general, it would be possible to adapt all values in the code manually on a case-by-case basis—however, this defeats the purpose of having a high-level programming language. Without language support, programmers are forced to manually handle accuracy parameters by passing all such parameters to the main routine, which forwards the necessary ones to each subroutine. For example, in the case of the QPE algorithm:

```

function QPE( $\epsilon_{QPE}, \epsilon_{TE}, \epsilon_{QFT}, \epsilon_{R_{TE}}, \epsilon_{R_{QFT}}, U$ )
   $reg\_size \leftarrow f(\epsilon_{QPE})$ 
  for  $i \leftarrow 0$  to  $reg\_size$  do
    for  $j \leftarrow 0$  to  $n\_iter(i)$  do
       ${}^cU(\epsilon_{TE}, \epsilon_{R_{TE}})$ 
  AQFT $^\dagger(\epsilon_{QFT}, \epsilon_{R_{QFT}})$ 

```

where cU is the controlled version of U .

This programmer-unfriendly approach does not allow code reuse for resource estimation, as implementations of subroutines need to be adapted to the context in which they are used and, in particular, to the choice of accuracy parameters. For example, ${}^cU(\epsilon_{TE}, \epsilon_{R_{TE}})$ is implemented using a number of Clifford+ T gates that depends on the chosen accuracy parameters.

When using our methodology, programmers only need to worry about accuracy parameters in subroutines where the corresponding errors are introduced. The compiler will take care of extracting all dependencies. Specifically, this allows us to express the pseudo-code for phase estimation as follows:

<pre> function cR declare ϵ_R ... function cU declare ϵ_{TE} ... function AQFT† declare ϵ_{QFT} $l \leftarrow g(\epsilon_{QFT})$ for $i \leftarrow 0$ to $g'(l)$ do ... ${}^cR()$... </pre>	<pre> function QPE(U) declare ϵ_{QPE} $reg_size \leftarrow f(\epsilon_{QPE})$ for $i \leftarrow 0$ to reg_size do for $j \leftarrow 0$ to $n_iter(i)$ do ${}^cU()$ AQFT$^\dagger()$ </pre>
---	--

Using abstract syntax tree (AST) transformations, our methodology is able to handle various levels of granularity, from using the same value for all accuracy parameters to using a different value for every instance that is created during runtime (via an accuracy parameter data structure that mirrors the call graph). This is crucial as there is a substantial trade-off between the number of accuracy parameters being considered and the resulting gate count [17]. This can be illustrated with the following example:

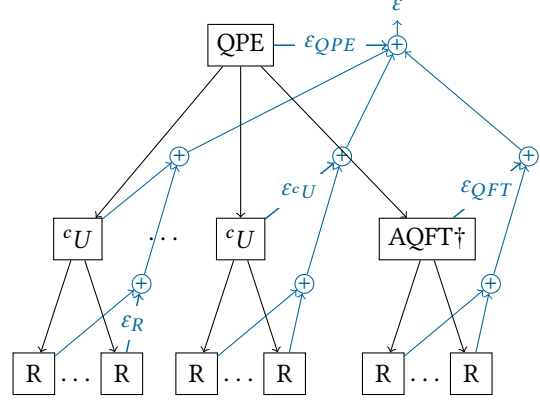


Figure 4. Flow diagram explaining how the code of the QPE algorithm is transformed into a code evaluating the overall approximation error ϵ .

Example 4. Consider Beauregard’s implementation of Shor’s algorithm [5]. In addition to the (semi-classical) inverse Fourier transform of phase estimation, every addition circuit requires two (approximate) QFTs [10] (one inverted, one regular) [12]. While the number of additions (and thus the number of QFTs) varies with the bit-size n of the number to factor, phase estimation always requires a single QFT. Therefore, it is natural to choose a different accuracy parameter for the (approximate) QFT of the phase estimation than for the (approximate) QFTs of the $O(n^2)$ -many n -bit additions.

Besides facilitating accuracy-aware implementations of quantum programs and providing various levels of granularity for assigning accuracy parameters, our methodology allows us to automatically deduce the number of contexts in which a given (approximate) decomposition is applied. This enables automatic selection of the number of accuracy parameters and thus removes the need to perform this task manually.

5 Automatic accuracy management

In this section, we describe the proposed procedure to automatically determine accuracy parameters. The optimization problem is solved using a simulated annealing procedure that iteratively changes the parameters and evaluates the corresponding total approximation error. The procedure terminates as soon as accuracy parameters have been found that guarantee a user-specified overall accuracy. To further improve the parameter selection, we also evaluate the circuit cost in terms of the T -count and pass the information to the optimization procedure. The result is a valid distribution of the available approximation error, which also aims to minimize the circuit cost.

Our approach is to extract a (near-)symbolic expression for the total error and gate count from the algorithm and use the obtained expressions in the annealing procedure. In

general, it is possible to use the annealing procedure with any available resource estimation method, the difference being that the runtime of each evaluation depends on the problem size if non-symbolic methods are used.

5.1 Cost/constraint functions: extraction

Our methodology proceeds by automatically generating two pieces of code that compute (an upper bound on) (i) the number of costly quantum gates (i.e., T gates) and (ii) the overall approximation error as a function of the different approximation errors. We denote the two functions by

$$T(\varepsilon_1, \dots, \varepsilon_n) \quad \text{and} \quad E(\varepsilon_1, \dots, \varepsilon_n).$$

The automatic generation of these two functions can be achieved via a few simple transformations of the program’s AST. Specifically, to generate T , all calls to native operations are removed from the AST, except those corresponding to costly gates that are replaced by counter-increments. The program computing a bound on the overall approximation error (E) can be generated in a similar fashion, where increments are added for every epsilon declaration (see Sec. 2.3).

Example 5. In Fig. 4 we show the different decomposition levels of the QPE algorithm. The standard coherent QPE requires $2^{n_{QPE}} - 1$ controlled time-evolution unitaries cU , followed by an inverse QFT. At the next decomposition level, each unitary (including the QFT) is decomposed into rotation gates. In turn, those rotations will be fed into rotation synthesis, which outputs a sequence of $\mathcal{O}(\log \frac{1}{\varepsilon_R})$ Clifford+ T gates for each rotation, where ε_R denotes the target accuracy of rotation synthesis (per rotation). Since errors accumulate at most linearly due to being unitary (see Sec. 2.3), an upper bound on the overall approximation error can be computed by adding all the ε_i introduced by the various decomposition steps.

5.2 Cost/constraint functions: optimization

Once the two pieces of code evaluating the total approximation error $E(\varepsilon_1, \dots, \varepsilon_n)$ and the cost $T(\varepsilon_1, \dots, \varepsilon_n)$ have been generated, they could be fed into the simulated annealing procedure. While this would allow us to perform accuracy management *automatically*, the resulting code will take substantial time to execute: typical quantum applications require on the order of 10^{15} or more operations [31] and the optimization loop is executed hundreds of times until suitable accuracy parameters are found.

As a remedy, we employ custom compiler optimization passes, which enable much faster evaluation of gate counts and error bounds. Specifically, our methodology aims to infer symbolic and loop-free expressions for (upper bounds on) gate count and overall approximation error. The following example demonstrates how beneficial the use of our symbolic approach is:

Example 6. Consider the example of the approximate quantum phase estimation algorithm and a two-mode simulated annealing procedure. Even with an optimized annealing schedule, it will require a minimum of about 200 evaluations to guarantee an overall approximation error of at most 10^{-2} . As accuracy parameters $\varepsilon_1 \dots \varepsilon_n$ approach the optimal values (minimizing the T -count), one evaluation of the non-optimized $T(\varepsilon_1, \dots, \varepsilon_n)$ function on 8 qubits takes 9m 10s, while evaluating the inferred symbolic expression takes 0.1 μ s. If the number of qubits grows to 16, then we have 34m 14s for the non-optimized case, while evaluating the expression still takes 0.1 μ s.

The transformations that we propose to implement at the intermediate-representation level of the compilation procedure are shown in Table 1. In particular, our optimization routine would:

1. Check if there is an addition between a variable v initialized outside the loop and a loop invariant, and if v is not used elsewhere in the loop. If so, apply transformation 1, where N is the number of iterations of the loop.
2. Check if there is an addition between a variable v initialized outside the loop and a function f only depending on the inductive variable and other loop invariants. If so, apply transformation 2. In the particular case where $f(i)$ is $\min()$, the expression can be upper bounded as shown in the table. In addition, polynomial expressions can be derived from some finite series using Faulhaber’s formula.
3. When generic branching instructions are found, they are transformed into $\max(\text{if}, \text{else})$ instructions, where the branch that gives the largest contribute to the cost function is selected.

The following example shows the described transformations applied to the AQFT quantum algorithm.

Example 7. The pseudo-code of the function $AQFT_T$, which computes the total number of T gates required for the AQFT algorithm, obtained after source-to-source transformation is shown in Alg. 1. As our implementation uses three rotation gates for each controlled-rotation, the function takes as input three accuracy parameters. This is why there are three innermost loops in Alg. 1. Since we want to extract a symbolic expression for the variable T_{count} , we have to get rid of as many loops as possible. The *if* statement is hoisted in the second loop, which becomes:

```
for j ← 0 to min(n - 1 - i, l) do
```

Then all the loops are optimized applying the transformations in Table 1. Finally, the code in Alg. 2 is obtained, which shows the closed-form expression for the T_{count} with respect to the algorithm’s parameters.

While our methodology succeeds at extracting closed-form expressions for all our examples, we note that this is not necessary for our methodology to work: The remaining

Table 1. Compiler transformations.

	Original Code	Symbolic expression
1	for $i \leftarrow 0$ to N do $v += \text{const}$	$v += \text{const} \cdot N$
2	for $i \leftarrow 0$ to N do $v += f(i)$	$v += \sum_i f(i)$
	for $i \leftarrow 0$ to N do $v += \min(g(i), h(i))$	$v += \sum_i \min(g(i), h(i))$
		\leq
	for $i \leftarrow 0$ to N do $v += \min(g(i), h(i))$	$v += \min(\sum_i g(i), \sum_i h(i))$
	for $i \leftarrow 0$ to N do $v += i^p$	$v += \sum_i i^p$ <small>$(p + 1)^{th}$ degree polynomial derived from Faulhaber's formula</small>
3	if (...) then expr1 else expr2	$\max(\text{expr1}, \text{expr2})$

control flow would not affect applicability or correctness, but merely cause an increase in runtime.

6 Compiler Requirements

In order to add the proposed accuracy management feature to any quantum programming language, it is necessary to integrate it into the language compiler. Here we describe all the features that the compiler must support. Meanwhile, we explain how the respective features are implemented in our two prototypes (LLVM and Q#).

6.1 Don't-cares

Our methodology requires that the compiler identifies subroutine parameters that have no, or a negligibly small, effect on either of the two functions being evaluated. The function will be called using the default value of the don't-care parameter as its argument. This allows the compiler to simplify repeated calls to the same function.

Example 8. *As a simple example, consider AQFT. Calls to functions with different parameters will have to be evaluated several times. For example, the function describing a rotation gate will take the rotation angle as a parameter. Nevertheless, the angle will have no impact on the approximation error selected to decompose the rotation. If several rotation gates are applied in the same algorithm with different angles, the corresponding calls will be evaluated several times by the compiler. We address this problem by annotating the angle parameter as a don't-care. This will result in many identical calls to the function with identical arguments that hence may be removed by the compiler.*

In our LLVM implementation, we use compiler annotations to introduce additional information in the source code. In particular, we attach a *don't-care* annotation to a parameter declaration if it has negligible effect on the cost/constraint functions.

6.2 Epsilon-declarations

To provide language support (see Section 4) the compiler must be capable of locating all introduced accuracy parameters. This can be done by matching against a specific class or by using annotations. In both our implementations, we match to declarations with a custom type. As the applied solutions are equivalent, we only detail the Q# solution, a language the reader is probably less familiar with.

Q#. Q# provides user-defined types by means of named types. We declare a user-defined type

```
newtype EpsilonValue = Double;
```

which allows the programmer to declare and use accuracy parameters, e.g.,

```
let eps_R = EpsilonValue(0.1);  
for (i in 1..Ceiling(1.5 * Lg(1.0 / eps_R!))) {  
    ...  
}
```

In the code, the epsilon value of 0.1 is just a dummy value, since the compiler requires the specification of a value. Further, the '!' postfix operator unwraps the value of the user-defined type into a value of type Double.

6.3 AST modification

The compiler must provide access to the AST and allow rewriting and copying. In particular, we need to generate 3 different versions of the entire program: one that computes the total approximation error, one that computes the total cost, and the original quantum program, which will ultimately be invoked using optimized accuracy parameters.

LLVM. We approach the problem of modifying the AST using source-to-source transformation. We implement a *Clang-Tool* and run an *ASTFrontendAction*: a routine that has access to the AST and allows us to interface with the source code. Our *ClangTool* outputs files containing the function to compute the T -count, e.g., the one in Alg. 1, and the function computing the total approximation error E . Our action exploits the *ASTmatcher* library, which allows us to match nodes in the AST that have some specific properties. The library provides a concise way of describing patterns and is implemented as a *domain-specific language* (DSL). In addition, matchers allow us to access to the source code by running a callback function on the matched AST nodes. Once the locations of interest in the code have been identified, we can use an instance of the *Rewriter* class to modify it accordingly. The AST being constant by design, we must generate a new file containing our transformed source code.

Our tool also makes use of header files in which we define basic quantum operations, such as the one in the Clifford+ T gate set. Those header files can be adjusted according to the specific application. For example, in addition to the T -gate, we might want to consider other expensive operations.

Finally, the tool adds to all function declarations the attribute *always inline* to enable successive optimization steps.

The result of running the Clang tool is a new source file computing the total error or gate count as a function of all the accuracy parameters defined in the source code.

Q#. We have implemented an AST transformation pass to detect all `EpsilonValue` declarations, remove them, and add them as arguments to the operation signature. This step is performed before producing the two pieces of code that compute the number of costly quantum gates and the upper bound on the overall approximation error.

There exist no global variables and no call-by-reference parameters in Q#. However, it is possible to declare an operation in Q# and implement it in C#. In order to count the number of T gates, we introduce an operation `IncrementCounter(id, value)` whose implementation in C# increments a global counter, called `id`, by `value`.

We use a similar technique as used for counting gates to accumulate the bound on the overall approximation error. Each declaration of an epsilon value is replaced by a call to an operation `IncrementValue(id, value)` whose implementation in C# increments a global variable called `id` by `value`.

The programs obtained after the described AST modifications could already be used to estimate the resource requirements of the quantum program. In this case, the only advantage with respect to using state-of-the-art methods would be that our approach provides language support by keeping track of all the introduced approximation errors, work that otherwise would have to be performed manually. In addition, the estimation would be too slow to be used in the simulated annealing procedure (see results in Fig. 5). To overcome this issue, the rewrites described in the following Section 6.4 are necessary to obtain estimates suited to be used to solve the optimization problem.

6.4 Rewrites to make evaluation more efficient

In order to speed up the optimization process, we need fast evaluations of the cost and error functions. The two functions extracted from most quantum algorithms will feature many loops performing simple counter increments or floating-point additions. Our goal is to extract a symbolic expression from the control flow structure. To this end, we employ loop optimization.

LLVM. We implemented compiler optimization passes with the purpose of eliminating loops in our cost estimate by transforming them into additions and multiplications. For example, the first loop optimization described in Table 1 needs to be performed for both integral and floating-point numbers, as approximation errors require double precision. We use an LLVM *loop pass* to perform this optimization.

Example 9. Consider the following code that computes the total approximation error of n quantum operations, characterized by the same approximation error `val`:

```
double Eps = 0.00;
double val = 0.02;
for (int i = 0; i < n; i++) {
    Eps += val;
}
```

Once this function is compiled into *Intermediate Representation (IR)* code, `val` will be identified as a loop-invariant variable, while `Eps` will be assigned to a so-called PHI node. PHI nodes assign a variable with a different value, depending on the predecessor of the current block. Where blocks are groups of instructions. In our example the PHI node would have two incoming values: 0.00 (if the predecessor block is outside the loop) and the temporary value containing the addition result (if the predecessor was the previous loop iteration). PHI nodes are defined in the loop header block.

The loop pass traverses the code from the innermost to the outermost loop in the IR and checks whether:

1. it contains an instruction performing the addition operation between a loop-invariant operand and a variable defined through a PHI node in the loop header,
2. the PHI node is only used in the addition operation inside the loop or in the loop latch block,
3. the result of the addition is only used as the incoming value of the PHI node.

If the described conditions apply, the loop is removed. Referring to the code in Example 9, the operations `%1 = val * n` and `%2 = Eps + %1` would be added to the pre-header loop block, i.e., outside the loop. In addition, the result `%2` would replace all uses of the original addition operation, which would be erased. All the other transformations in Table 1 are achieved in a similar fashion.

Q#. The Q# compiler already contains some transformation passes, e.g., for operation inlining, propagating constants, or removing unused code. We have added two additional transformation passes that optimize the use of `IncrementCounter` and `IncrementValue` calls. Without loss of generality we explain the transformation passes by means of the `IncrementCounter` operation, remarking that they work analogously for the `IncrementValue` operation.

The first transformation pass collects all `IncrementCounter` calls inside a scope level that have the same `id` and do not contain values incorporating mutable variables. These calls can be merged into a single call by accumulating all values, benefiting from further optimization, e.g., constant propagation. The second transformation pass lifts `IncrementCounter` calls inside a `for`-loop. If the call is the only statement in the body of the `for`-loop and does not use the loop variable to compute the value, the `for`-loop can be removed when multiplying the value in the `IncrementCounter` call by the number of loop iterations.

Algorithm 1 Cost function for the AQFT algorithm

```
function N_ROT( $\epsilon_{rot}$ ) return  $1.5 * \log_2(1./\epsilon_{rot})$ 
function AQFT_T( $\epsilon_{QFT}, \epsilon_{R_1}, \epsilon_{R_2}, \epsilon_{R_3}$ )
   $T_{count} \leftarrow 0$ 
   $l \leftarrow \lceil \log_2(n/\epsilon_{QFT}) \rceil + 3$ 
  for  $i \leftarrow 0$  to  $n$  do
    for  $j \leftarrow 0$  to  $n - 1 - i$  do
      if  $j \leq l$  then
        for  $k \leftarrow 0$  to  $N\_ROT(\epsilon_{R_1})$  do  $T_{count}++$ 
        for  $k \leftarrow 0$  to  $N\_ROT(\epsilon_{R_2})$  do  $T_{count}++$ 
        for  $k \leftarrow 0$  to  $N\_ROT(\epsilon_{R_3})$  do  $T_{count}++$ 
  return  $T_{count}$ 
```

Algorithm 2 Cost function for the AQFT algorithm after loop optimization

```
function AQFT_T( $\epsilon_{QFT}, \epsilon_{R_1}, \epsilon_{R_2}, \epsilon_{R_3}$ )
   $T_{count} \leftarrow 0$ 
   $l \leftarrow \lceil \log_2(n/\epsilon_{QFT}) \rceil + 3$ 
   $T_{count} = T_{count} + \min(\frac{n(n-1)}{2}, nl) \cdot (N\_ROT(\epsilon_{R_1}) + N\_ROT(\epsilon_{R_2}) + N\_ROT(\epsilon_{R_3}))$ 
  return  $T_{count}$ 
```

Extraction of symbolic representation. Our LLVM prototype also has a method that navigates the fully optimized IR code and extracts symbolic expressions for the two estimates.

LLVM. The pass to extract the symbolic expression from the IR has been implemented as an LLVM *function pass*. Given the main function, it starts from the return instruction and recursively visits all instruction’s operands annotating the respective functionality. The recursion terminates when the operand is a constant or, in general, is not an instruction.

The extraction pass supports the following instructions: casting, PHI nodes, selects, truncations, zero extensions, call instructions, compare instructions, shifts, addition, multiplication, division, and subtraction. The expression is written in the Wolfram language, such that Mathematica [20] can be used for conversion to \LaTeX and further expression simplifications.

7 Qualitative evaluation

In this section, we evaluate our prototypes using different quantum algorithms. Starting with a simple quantum Fourier transform, we increase the complexity of our examples. As a highlight, we extract a symbolic expression for the phase estimation of a Trotter-decomposed time-evolution under a transverse-field Ising model Hamiltonian, where the phase estimation features an approximate QFT. The complete pseudo-code for this algorithm is shown in Alg. 5. In addition, we also tested our tool on Shor’s algorithm [33], to provide the reader with a large-scale example. We used the period finding quantum routine as implemented in the

Algorithm 3 Exact QFT algorithm

```
function QFT( $qubits$ )
  for  $i \leftarrow 0$  to  $n$  do
    H( $qubits[i]$ )
    for  $j \leftarrow 0$  to  $n - i - 1$  do
       $control = qubits[j + 1 + i]$ 
       $angle = \pi/(j + 1)^2$ 
       $target = qubits[i]$ 
      controlled_R( $control, angle, target$ )
```

Algorithm 4 AQFT algorithm

```
function AQFT( $qubits$ )
  declare  $\epsilon_{QFT}$ 
   $\leftarrow \lceil \log_2(n/\epsilon_{QFT}) \rceil + 3$ 
  for  $i \leftarrow 0$  to  $n$  do
    H( $qubits[i]$ )
    for  $j \leftarrow 0$  to  $n - i - 1$  do
      if  $j \leq l$  then
         $control = qubits[j + 1 + i]$ 
         $angle = \pi/(j + 1)^2$ 
         $target = qubits[i]$ 
        controlled_R( $control, angle, target$ )
```

open source programming framework ProjectQ [34]. Our prototype leverages Wolfram/Mathematica [20] to export the resulting expression to \LaTeX .

Exact QFT. The first example is the QFT algorithm, described in Alg. 3. Our implementation is able to directly optimize all loops, including the outermost loop which yields a sum of the form $\sum_i i = \frac{n(n-1)}{2}$. The expressions for T -count and total approximation error are:

$$T \simeq 3.246n(n-1) \log \left(\frac{1}{\epsilon_R} \right)$$
$$E = \frac{3}{2} \epsilon_R n(n-1)$$

Approximate QFT (AQFT). Next, we consider the approximate QFT, implemented in Alg. 4. An intermediate expression of the form $c + \sum_i \min(f(i), g(i))$ is upper bounded by choosing one of the arguments to the min-function. Our prototype implementation returns the following expressions:

$$T \simeq 6.492n \log \left(\frac{1}{\epsilon_R} \right) \left(\left\lceil \frac{\log(\frac{n}{\epsilon_{QFT}})}{\log 2} \right\rceil + 3 \right)$$
$$E \simeq 3\epsilon_R n \left(\left\lceil \frac{\log(\frac{n}{\epsilon_{QFT}})}{\log 2} \right\rceil + 3 \right) + \epsilon_{QFT}$$

Quantum phase estimation (QPE). We combine the time evolution of a TFIM with QPE, to find the ground state of the TFIM. The pseudo-code is shown in Alg. 5. A simplifying

Algorithm 5 QPE algorithm

```

function CTE(control_qubit, qubits)
  declare  $\epsilon_{TE}$ 
   $n\_steps = 1/\sqrt{\epsilon_{TE}}$ 
  for  $i \leftarrow 0$  to  $n\_steps$  do
    for  $j \leftarrow 0$  to  $n - 1$  do
      target = qubits[j + 1]
      CNOT(qubits[j], target)
      controlled_Rz(control_qubit, 1.0, target)
      CNOT(qubits[j], target)
    for  $j \leftarrow 0$  to  $n$  do
      target = qubits[j]
      H(target)
      controlled_Rz(control_qubit, 2.0, target)
      H(target)
function QPE(qubits)
  declare  $\epsilon_{QPE}$ 
   $reg\_size \leftarrow \lceil -\log_2(\epsilon_{QPE}/(2 * \pi)) \rceil + 2$ 
  for  $i \leftarrow 0$  to  $reg\_size$  do
    control = reg[i]
     $n\_iter \leftarrow 2^i$ 
    H(control)
    for  $j \leftarrow 0$  to  $n\_iter$  do
      CTE(control, qubits)
  AQFT†(reg)
  
```

assumption we made in this first QPE example is that the inverse QFT can be performed natively. Our methodology successfully removes all loops. The resulting expressions for the total error and the T -count are:

$$T \simeq \frac{34.625 (n - \frac{1}{2}) \log\left(\frac{1}{\epsilon_R}\right) \left(2^{\lceil 2.652 - 1.443 \log(\epsilon_{QPE}) \rceil - \frac{1}{4}}\right)}{\sqrt{\epsilon_{TE}}}$$

$$E \simeq \frac{\left(\epsilon_R(n - \frac{1}{2}) + \frac{\epsilon_{TE}^{3/2}}{4}\right) \left(2^{\lceil 2.652 - 1.443 \log(\epsilon_{QPE}) \rceil + 4} - 4\right)}{\sqrt{\epsilon_{TE}}} + \epsilon_{QPE}$$

Dropping the simplifying assumption from the previous example, we implement the inverse QFT as in Section 3.2. The updated expressions for T -count and total error are:

$$T \simeq \log\left(\frac{1}{\epsilon_R}\right) \left(\frac{(n - \frac{1}{2})(34.625^{\lceil 2.652 - 1.443 \log(\epsilon_{QPE}) \rceil} - 8.656)}{\sqrt{\epsilon_{TE}}} + \left[2.652 - 1.443 \log(\epsilon_{QPE})\right](3.246^{\lceil 2.652 - 1.443 \log(\epsilon_{QPE}) \rceil} + 9.738) + 6.492 \right)$$

$$E \simeq \frac{16 \left(\epsilon_R \left(n - \frac{1}{2} \right) + \frac{\epsilon_{TE}^{3/2}}{4} \right) \left(2^{\lceil 2.652 - 1.443 \log(\epsilon_{QPE}) \rceil} - \frac{1}{4} \right)}{\sqrt{\epsilon_{TE}}} + \frac{3}{2} \epsilon_R \left(\lceil 2.652 - 1.443 \log(\epsilon_{QPE}) \rceil + 1 \right) \left(\lceil 2.652 - 1.443 \log(\epsilon_{QPE}) \rceil + 2 \right) + \epsilon_{QPE}$$

Finally, we replace the exact QFT by an approximate QFT (see Alg. 4). Again, our optimization pass can upper bound an intermediate expression of the form $c + \sum_i \min(f(i), g(i))$ by choosing one of the arguments to the min-function:

$$T \simeq \log\left(\frac{1}{\epsilon_R}\right) \left(6.492 \left(\lceil 2.652 - 1.443 \log(\epsilon_{QPE}) \rceil + 2 \right) \left(\left\lceil \frac{\log\left(\frac{\lceil 2.652 - 1.443 \log(\epsilon_{QPE}) \rceil + 2}{\epsilon_{QFT}}\right)}{\log 2}\right\rceil + 3 \right) + \frac{34.625 \left(n - \frac{1}{2} \right) \left(2^{\lceil 2.652 - 1.443 \log(\epsilon_{QPE}) \rceil} - \frac{1}{4} \right)}{\sqrt{\epsilon_{TE}}} \right)$$

$$E \simeq 3\epsilon_R \left(\lceil 2.652 - 1.443 \log(\epsilon_{QPE}) \rceil + 2 \right) \left(\left\lceil \frac{\log\left(\frac{\lceil 2.652 - 1.443 \log(\epsilon_{QPE}) \rceil + 2}{\epsilon_{QFT}}\right)}{\log 2}\right\rceil + 3 \right) + \frac{16 \left(\epsilon_R \left(n - \frac{1}{2} \right) + \frac{\epsilon_{TE}^{3/2}}{4} \right) \left(2^{\lceil 2.652 - 1.443 \log(\epsilon_{QPE}) \rceil} - \frac{1}{4} \right)}{\sqrt{\epsilon_{TE}}} + \epsilon_{QFT} + \epsilon_{QPE}$$

Shor's algorithm. As last example, we present the results for Beauregard's implementation of Shor's algorithm [5], which defines two approximation errors, one for the rotation gates ϵ_R and one for the approximate QFT (ϵ_{QFT}). The resulting functions are:

$$T \simeq 2n^2 \left(129.843(n + 1) \log\left(\frac{1}{\epsilon_R}\right) \left\lceil \frac{\log\left(\frac{n+1}{\epsilon_{QFT}}\right)}{\log 2}\right\rceil + 471.761(n + 1) \log\left(\frac{1}{\epsilon_R}\right) + 84n + 91 \right)$$

$$E \simeq 4n^2 \left(\epsilon_R(n + 1) \left(30 \left\lceil \frac{\log\left(\frac{n+1}{\epsilon_{QFT}}\right)}{\log 2}\right\rceil + 109 \right) + 10\epsilon_{QFT} \right).$$

In summary, our methodology successfully produces closed-form expressions to compute the total error and gate count for all our examples. In the next section, we show the benefits of having access to symbolic expressions when optimizing accuracy parameters in terms of optimization runtime.

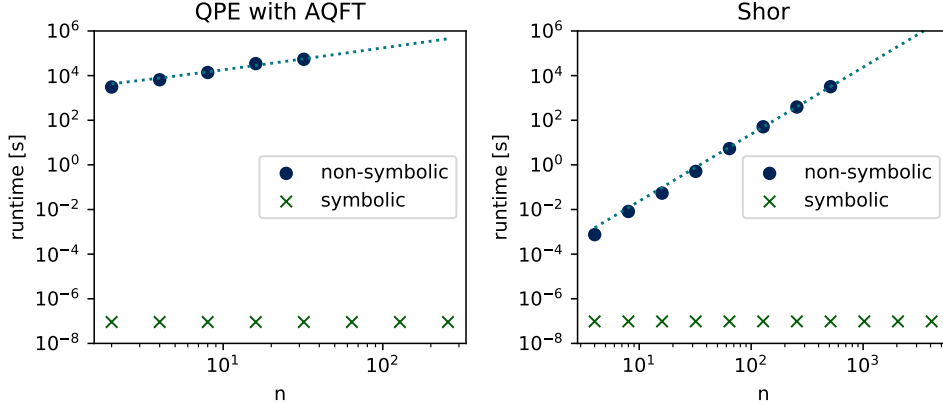


Figure 5. Each data point marks the runtime required for a single evaluation of the T function plus a single evaluation of the E function for the QPE algorithm with approximate QFT and for Shor’s algorithm. The accuracy parameters used are selected by the annealer procedure in order to bound the approximation error to $5 \cdot 10^{-3}$. A comparison between the runtimes of the non-symbolic approach and the symbolic approach developed in this paper is shown. We provide polynomial extrapolations from the collected runtimes for the non-symbolic approach as the runtime tops out for bit sizes above 512 for Shor and 32 for QPE.

8 Quantitative evaluation

In this section, we demonstrate how our code, optimized using the transformations in Table 1, enables faster evaluations of the cost/constraint functions. We compare the runtimes of our symbolic resource estimation method against a *non-symbolic* approach. The latter does not use symbolic estimations for resources and errors. The non-symbolic estimates are generated by our prototypes during the AST modification step (see Section 6.3).

We ran all experiments on a MacBook Pro with an Intel Core i5 processor with 3.1 GHz processor clock frequency and 16 GB main memory. All source codes have been compiled using Clang version 9.0.0 with level 3 optimization (`-O3`) and with the fast-math mode enabled (`-ffast-math`).

For these experiments, we select our Clang/LLVM prototype. As previously described, it uses a two-mode annealing procedure to find suitable assignments for all accuracy parameters. We measure the runtime for performing one evaluation of the T and E functions using accuracy parameters provided by the annealer, guaranteeing an upper bound on the overall approximation equal to $5 \cdot 10^{-3}$. The runtime measurements are performed using different input sizes for Shor’s algorithm and for our QPE example (with approximate QFT). The plots in Fig. 5 depict the sum of the runtimes required for evaluating the constraint and cost functions once, as they are always evaluated the same number of times in the simulated annealing procedure. While the non-symbolic approach exhibits a growing runtime as a function of the problem size, our symbolic method features the expected constant behavior. In particular, the runtime of the non-symbolic approach grows linearly for the QPE example and (roughly) cubically for our implementation of Shor’s algorithm.

Given that the QPE example is only interesting for $n \gg 50$ and the target number of bits for Shor’s algorithm is $n \approx 4000$, we show function extrapolations for the non-symbolic approach in Fig. 5. The two resulting functions are $f_{QPE} = 1737.30x + 816.98$ and $f_{Shor} = 2.38 \cdot 10^{-5}x^3$. We aim to provide an indication of how much time it would take for the non-symbolic approach to optimize accuracy parameters using our proposed methodology. We thus estimate the minimum number of evaluations of the functions T and E required for the annealer to converge to a good result. For our examples, this is between 200 and 400 evaluations, independent of problem size.

We may thus conclude that non-symbolic approaches are not feasible for large-scale applications: For example, if we multiply our runtime results in Fig. 5(b) for the number of evaluations required to find suitable accuracy parameters for Shor’s algorithm, we obtain a runtime of approximately 1890 days for $n = 4096$ bits and an overall approximation error of at most $5 \cdot 10^{-3}$.

9 Conclusion and outlook

We describe the first framework with the ability to automatically manage approximation errors and outputting (near-)symbolic resource estimates.

Our methodology can be added to any quantum software framework, thereby greatly facilitating resource estimation of quantum programs. Such integration will allow even domain-experts from, e.g., chemistry or machine learning, to write accuracy-aware quantum programs without having to manually derive and prove error bounds.

In this work, we identify the features that a quantum programming language must support in order to enable our

methodology. We develop two prototype implementations, which we evaluate on various example programs.

Future work could implement improved handling of branching on measurement results and repeat-until-success-like structures. To handle such programs, our methodology requires additional input such as the maximal or expected iteration count (e.g., as a program annotation). For verification purposes, one could instrument the code in order to assert that the actual number of iterations does not deviate (too much) from the provided estimate. Future work could also compare upper bounds to actually achieved errors on example applications. Currently, our methodology doesn't take into account gate cancellations that may be performed by circuit optimization. This, in addition to the repeated use of the triangle inequality to bound the overall error, likely leads to pessimistic error bounds.

References

- [1] Matthew Amy, Dmitri Maslov, Michele Mosca, and Martin Roetteler. 2013. A Meet-in-the-Middle Algorithm for Fast Synthesis of Depth-Optimal Quantum Circuits. *IEEE Transactions on Computer-Aided Design of Integrated Circuits and Systems* 32, 6 (Jun 2013), 818–830. <https://doi.org/10.1109/tcad.2013.2244643>
- [2] Thanassis Avgerinos, Alexandre Rebert, Sang Kil Cha, and David Brumley. 2014. Enhancing symbolic execution with veritesting. In *36th International Conference on Software Engineering, ICSE '14*. 1083–1094. <https://doi.org/10.1145/2568225.2568293>
- [3] Ryan Babbush, Dominic W. Berry, Yuval R. Sanders, Ian D. Kivlichan, Artur Scherer, Annie Y. Wei, Peter J. Love, and Alán Aspuru-Guzik. 2017. Exponentially more precise quantum simulation of fermions in the configuration interaction representation. *Quantum Science and Technology* 3, 1 (2017), 015006.
- [4] Earl T. Barr, Thanh Vo, Vu Le, and Zhenqiang Su. 2013. Automatic detection of floating-point exceptions. In *ACM Sigplan Notices*, Vol. 48. ACM, 549–560.
- [5] Stephane Beauregard. 2002. Circuit for Shor's algorithm using $2n+3$ qubits. *arXiv preprint quant-ph/0205095* (2002).
- [6] Charles H. Bennett and Gilles Brassard. 2014. Quantum cryptography: public key distribution and coin tossing. *Theor. Comput. Sci.* 560, 12 (2014), 7–11.
- [7] Sylvie Boldo. 2008. Kahan's algorithm for a correct discriminant computation at last formally proven. *IEEE Trans. Comput.* 58, 2 (2008), 220–225.
- [8] Sergey Bravyi and Alexei Kitaev. 2005. Universal quantum computation with ideal Clifford gates and noisy ancillas. *Physical Review A* 71 (Feb 2005), 022316. Issue 2. <https://doi.org/10.1103/PhysRevA.71.022316>
- [9] Earl T. Campbell and Mark Howard. 2017. Unified framework for magic state distillation and multiqubit gate synthesis with reduced resource cost. *Physical Review A* 95, 2 (Feb 2017). <https://doi.org/10.1103/physreva.95.022316>
- [10] Don Coppersmith. 2002. An approximate Fourier transform useful in quantum factoring. (2002). [arXiv:quant-ph/0201067](https://arxiv.org/abs/quant-ph/0201067)
- [11] Eva Darulova and Viktor Kuncak. 2014. Sound compilation of reals. In *Acm Sigplan Notices*, Vol. 49. ACM, 235–248.
- [12] Thomas G. Draper. 2000. Addition on a quantum computer. *arXiv preprint quant-ph/0008033* (2000).
- [13] Héctor Abraham et al. 2019. Qiskit: An Open-source Framework for Quantum Computing. (2019). <https://doi.org/10.5281/zenodo.2562110>
- [14] Simon Forest, David Gosset, Vadym Kliuchnikov, and David McKinnon. 2015. Exact synthesis of single-qubit unitaries over Clifford-cyclotomic gate sets. *J. Math. Phys.* 56, 8 (2015), 082201.
- [15] Austin G. Fowler, Matteo Mariantoni, John M. Martinis, and Andrew N. Cleland. 2012. Surface codes: Towards practical large-scale quantum computation. *Physical Review A* 86, 3 (Sep 2012). <https://doi.org/10.1103/physreva.86.032324>
- [16] Alexander S. Green, Peter LeFanu Lumsdaine, Neil J. Ross, Peter Selinger, and Benoît Valiron. 2013. Quipper: a scalable quantum programming language. In *ACM SIGPLAN Notices*, Vol. 48. ACM, 333–342.
- [17] Thomas Häner, Martin Roetteler, and Krysta M. Svore. 2018. Managing approximation errors in quantum programs. *arXiv preprint arXiv:1807.02336* (2018).
- [18] Vojtěch Havlíček, Antonio D. Córcoles, Kristan Temme, Aram W. Harrow, Abhinav Kandala, Jerry M. Chow, and Jay M. Gambetta. 2019. Supervised learning with quantum-enhanced feature spaces. *Nature* 567, 7747 (Mar 2019), 209–212. <https://doi.org/10.1038/s41586-019-0980-2>
- [19] Shih-Han Hung, Keshava Hietala, Shaopeng Zhu, Mingsheng Ying, Michael Hicks, and Xiaodi Wu. 2019. Quantitative robustness analysis of quantum programs. *Proceedings of the ACM on Programming Languages* 3, POPL (2019), 31:1–31:29. <https://doi.org/10.1145/3290344>
- [20] Wolfram Research, Inc. [n. d.]. Mathematica, Version 12.0. ([n. d.]). <https://www.wolfram.com/mathematica> Champaign, IL, 2019.
- [21] Ali Javadi-Abhari, Shruti Patil, Daniel Kudrow, Jeff Heckey, Alexey Lvov, Frederic Chong, and Margaret Martonosi. 2014. ScaffCC: a framework for compilation and analysis of quantum computing programs. *Proceedings of the 11th ACM Conference on Computing Frontiers, CF 2014* (05 2014). <https://doi.org/10.1145/2597917.2597939>
- [22] Alexei Kitaev. 1995. Quantum measurements and the Abelian Stabilizer Problem. *arXiv preprint arXiv:quant-ph/9511026* (1995).
- [23] Emmanuel Knill. 1996. *Conventions for quantum pseudocode*. Technical Report. Los Alamos National Lab., NM (United States).
- [24] Guang Hao Low and Isaac L. Chuang. 2019. Hamiltonian simulation by qubitization. *Quantum* 3 (2019), 163.
- [25] Sam McArdle, Suguru Endo, Alán Aspuru-Guzik, Simon Benjamin, and Xiao Yuan. 2018. Quantum computational chemistry. (2018). [arXiv:quant-ph/1808.10402](https://arxiv.org/abs/1808.10402)
- [26] Michael A. Nielsen and Isaac L. Chuang. 2002. *Quantum computation and quantum information*. (2002).
- [27] Adam Paetznick and Krysta M. Svore. 2013. Repeat-Until-Success: Non-deterministic decomposition of single-qubit unitaries. *arXiv preprint arXiv:1311.1074* (2013).
- [28] Pavel Panchekha, Alex Sanchez-Stern, James R. Wilcox, and Zachary Tatlock. 2015. Automatically improving accuracy for floating point expressions. In *ACM SIGPLAN Notices*, Vol. 50. ACM, 1–11.
- [29] Stefano Pirandola, Ulrik L. Andersen, Leonardo Banchi, Mario Berta, Darius Bunandar, Roger Colbeck, Dirk R. Englund, Tobias Gehring, Cosmo Lupo, Carlo Ottaviani, Jason Pereira, Mohsen Razavi, Jesni S. Shaari, Marco Tomamichel, Vladyslav C. Usenko, Giuseppe Vallone, Paolo Villoresi, and Petros Wallden. 2019. Advances in Quantum Cryptography. (2019). [arXiv:quant-ph/1906.01645](https://arxiv.org/abs/1906.01645)
- [30] David Poulin, Matthew B Hastings, Dave Wecker, Nathan Wiebe, Andrew C Doherty, and Matthias Troyer. 2014. The Trotter step size required for accurate quantum simulation of quantum chemistry. *arXiv preprint arXiv:1406.4920* (2014).
- [31] Markus Reiher, Nathan Wiebe, Krysta M. Svore, Dave Wecker, and Matthias Troyer. 2017. Elucidating reaction mechanisms on quantum computers. *Proceedings of the National Academy of Sciences* 114, 29 (2017), 7555–7560.
- [32] Artur Scherer, Benoît Valiron, Siun-Chuon Mau, Scott Alexander, Eric van den Berg, and Thomas E. Chapuran. 2017. Concrete resource analysis of the quantum linear-system algorithm used to compute the electromagnetic scattering cross section of a 2D target. *Quantum Information Processing* 16, 3 (Jan 2017). <https://doi.org/10.1007/s11128-016-1495-5>

- [33] Peter W. Shor. 1994. Algorithms for quantum computation: discrete logarithms and factoring. In *Proceedings 35th Annual Symposium on Foundations of Computer Science*. 124–134. <https://doi.org/10.1109/SFCS.1994.365700>
- [34] Damian S. Steiger, Thomas Hädner, and Matthias Troyer. 2018. ProjectQ: an open source software framework for quantum computing. *Quantum* 2 (Jan 2018), 49. <https://doi.org/10.22331/q-2018-01-31-49>
- [35] Martin Suchara, John Kubiawicz, Arvin I. Faruque, Frederic T. Chong, Ching-Yi Lai, and Gerardo Paz. 2013. QuRE: The Quantum Resource Estimator toolbox. In *2013 IEEE 31st International Conference on Computer Design, ICCD 2013*. 419–426. <https://doi.org/10.1109/ICCD.2013.6657074>
- [36] Krysta M. Svore, Alan Geller, Matthias Troyer, John Azariah, Christopher Granade, Bettina Heim, Vadym Kliuchnikov, Mariia Mykhailova, Andres Paz, and Martin Roetteler. 2018. Q#: Enabling Scalable Quantum Computing and Development with a High-level DSL. In *Real World Domain Specific Languages Workshop*. 7:1–7:10. <https://doi.org/10.1145/3183895.3183901>
- [37] Mingsheng Ying. 2009. Hoare Logic for Quantum Programs. (2009).